

A novel power conversion circuit for cost-effective battery-fuel cell hybrid systems[☆]

Dae-Kyu Choi^a, Byoung-Kuk Lee^{b,*}, Se-Wan Choi^c, Chung-Yuen Won^a,
Dong-Wook Yoo^b

^a *Sungkyunkwan University, Suwon, Republic of Korea*

^b *Korea Electrotechnology Research Institute, Power Electronics Group, Sungju-Dong 28-1, Changwon, Republic of Korea*

^c *Seoul National University of Technology, Seoul, Republic of Korea*

Received 17 December 2004; accepted 12 January 2005

Available online 12 April 2005

Abstract

The purpose of this paper is to develop a novel power conversion circuit for cost-effective battery-fuel cell hybrid systems. First of all, the various reduced parts power conversion systems (PCS) are overviewed and an advanced dc–dc boost converter and a bidirectional dc–dc converter are proposed. Theoretical explanation and informative simulation and experimental results are provided, along with the evaluation of the developed topologies in performance points of view.

© 2005 Elsevier B.V. All rights reserved.

Keywords: Battery-fuel cell hybrid; Power conversion system; dc–dc boost converter; Bidirectional dc–dc converter

1. Introduction

A fuel cell system mainly consists of a fuel cell stack, a fuel reformer, a fuel supplier (air management system), a power conditioning system (PCS), and a heat recovery system (HRS), as shown in Fig. 1. In order to commercialize the fuel cell system by year of 2010, the cost target is an important factor as well as its performance and reliability. From the evaluation of DOE, it sets the goal is to develop a ceramic fuel cell with factory costs as low as \$400 per kilowatt and today's fuel cells sell for well over \$4000 per kilowatt. If the cost targets can be met, future fuel cells could compete economically with virtually all types of power systems, including gas turbine and diesel generators. Basically in fuel cell systems, the fuel cell module overwhelms the majority of the entire cost of the system by over 50% and the rest shares the cost, such as reformer 20%, HRS 10%, PCS 15%,

and etc. 5%. Beside the effort of development of low-cost fuel cell stacks, one can find cost-effective solutions from PCS.

The PCS plays an important role to deliver the generating power from fuel cells to various loads according to end users' demands. Therefore, the PCS should be designed and operated with high efficiency, high performance, and high reliability, and especially low cost. The PCS consists of a dc–dc converter, a bidirectional dc–dc converter, and a dc–ac inverter, along with an energy storage unit. There are hundreds of PCS topologies in speed adjustable ac motor drives systems. However, these topologies are not optimally suitable for fuel cells because of unique nonlinear V – I static and dynamic characteristics of fuel cells. Moreover, it is a big challenge to design a low-cost PCS with high efficiency and performance.

The purpose of this paper is to develop a novel power conversion circuit, which is suitable for battery-fuel cell hybrid systems. The various reduced parts PCS topologies are overviewed and an advanced dc–dc boost converter and bidirectional dc–dc converter are proposed. Theoretical explanation and informative simulation and experimental results are

[☆] This paper was presented at the 2004 Fuel Cell Seminar, San Antonio, TX, USA.

* Corresponding author. Tel.: +82 55 280 1416; fax: +82 55 280 1436.

E-mail address: bklee@keri.re.kr (B.-K. Lee).

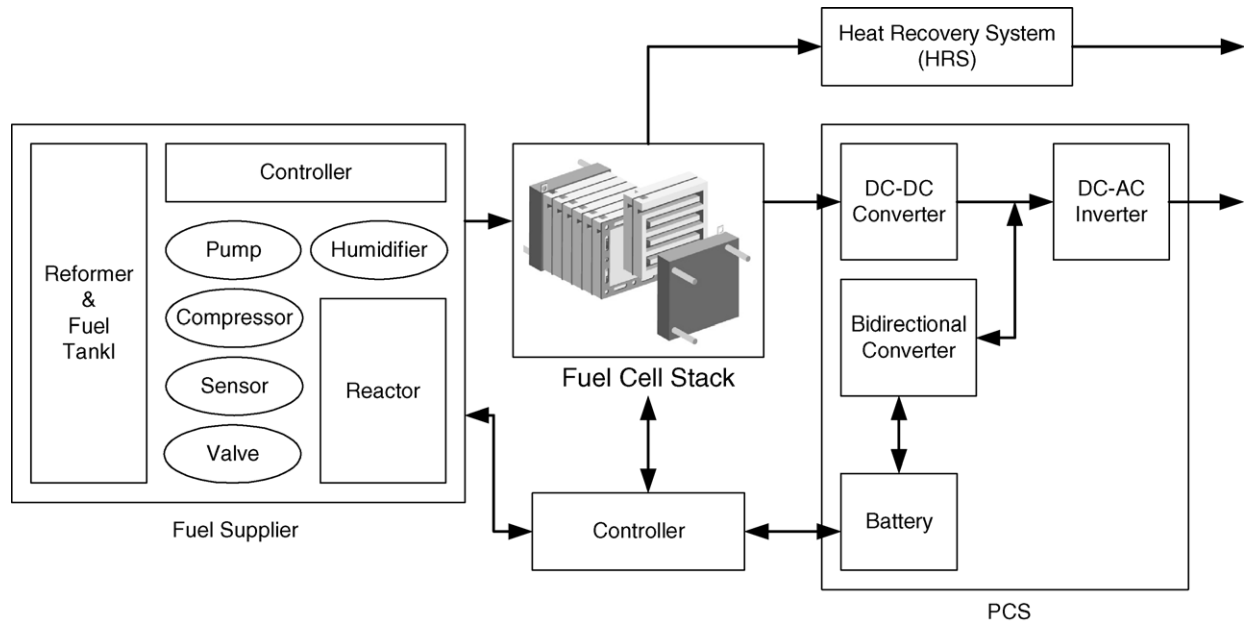


Fig. 1. Block diagram of a fuel cell generation system.

provided, along with the evaluation of the developed topologies in cost and performance points of view.

2. Basic characteristic consideration of fuel cell systems

2.1. Electrical characteristics of fuel cells

As shown in Fig. 2, a fuel cell outputs highly nonlinear $V-I$ characteristic. This curve can be represented as activation polarization, ohmic polarization, and concentration polarization, which can be obtained from the governing equations as

Eq. (1):

$$\begin{aligned}
 V &= E - \Delta V_{\text{ohm}} - \Delta V_{\text{act}} - \Delta V_{\text{concent}} \\
 &= E - ir - A \ln \left(\frac{i + i_n}{i_0} \right) + m \exp(ni) \\
 &= E_{\text{oc}} - ir - A \ln(i) + m \exp(ni)
 \end{aligned}
 \tag{1}$$

where E is the reversible OCV, i_n the fuel crossover, A the slope of Tafel line, i_0 the current density at the cathode, m and n the constants in the mass-transfer overvoltage, r the area-specific resistance [1].

Therefore, when one designs a PCS one should consider this nonlinear characteristic along with the power demands of the PCS. The operating points should be located within the ohmic polarization region in order to ensure the safe operation and also it should be noted that the entire efficiency of the PCS is changed according to the various operating points. Generally, in design of a PCS for a certain fuel cell, the power capacity of the PCS should be calculated as follows, assuming the single cell voltage is 0.8 V, the number of cells for the stack is 30, current density of the cell is 600 mA/cm², and area is 50 cm²:

- Power capacity of fuel cells
 - Voltage : 0.8 V/cell × 30 = 24 V,
 - current : 600 mA/cm² × 50 cm² = 30 A,
 - power = $V \times I = 24 \text{ V} \times 30 \text{ A} = 720 \text{ W}$
- Power capacity of PCS (overcurrent 150%)
 - Voltage (no-load) : 1.2 V/cell × 30 = 36 V,
 - current : 900 mA/cm² × 50 cm² = 45 A,
 - Power = $V \times I = 36 \text{ V} \times 45 \text{ A} = 1620 \text{ W}$

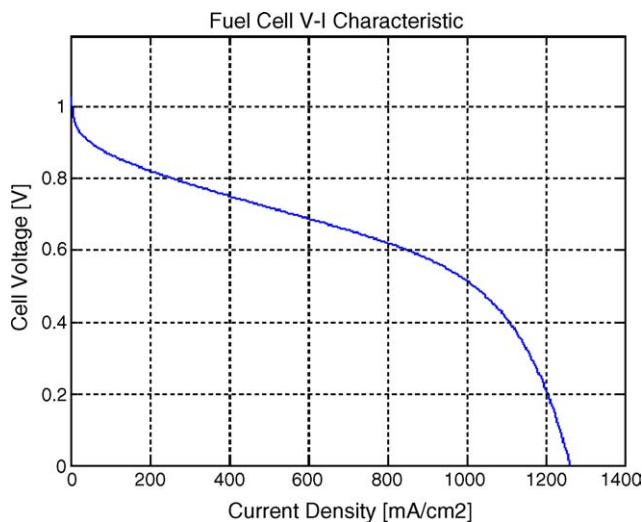


Fig. 2. $V-I$ characteristics of a fuel cell.

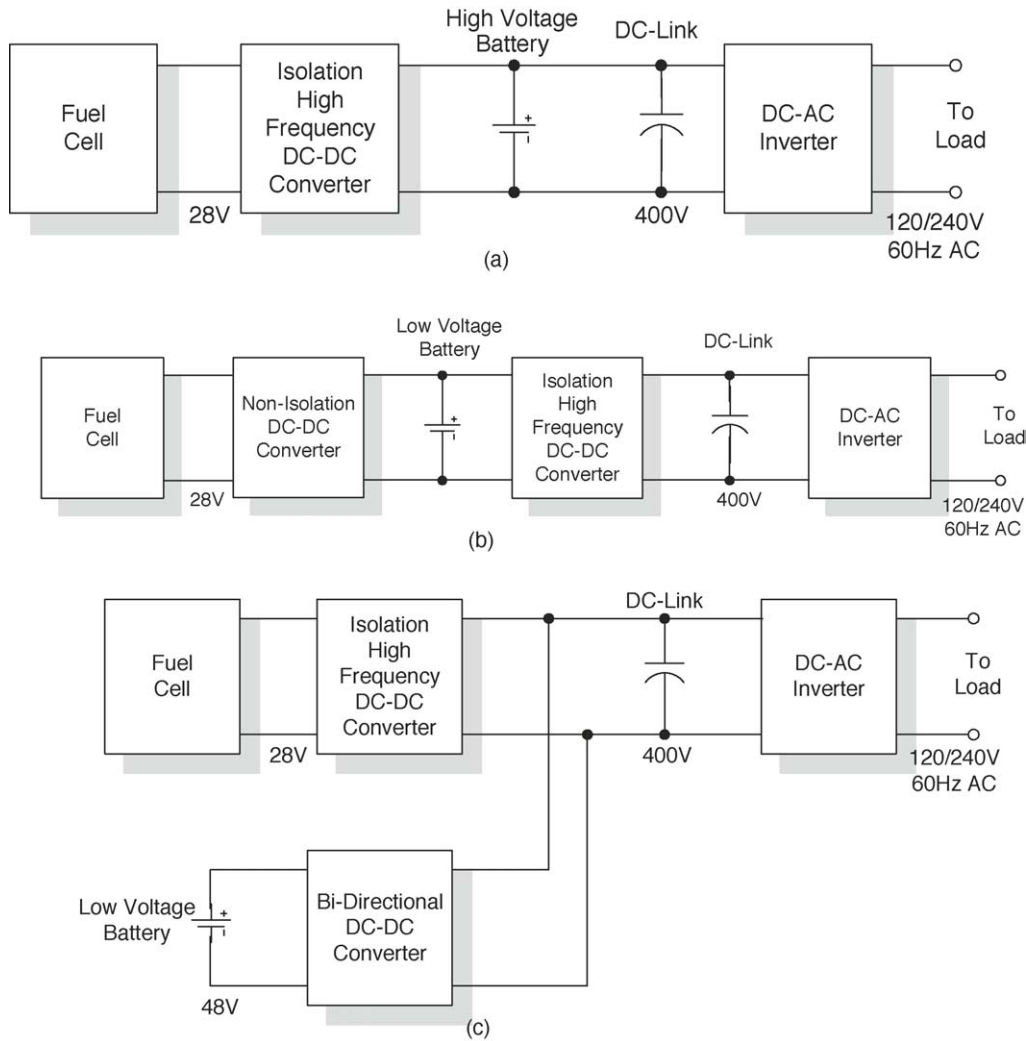


Fig. 3. Basic configurations of PCS for fuel cells: (a) type 1; (b) type 2 and (c) type 3.

2.2. Basic configurations of PCS [2,3]

The fuel cell is a kind of low-voltage and high-current energy source, so that the output voltage (28–42 V_{dc}) of fuel cell should be boosted up to about 400 V_{dc} before it converts into a 120/220 V, 60/50 Hz ac source. This boosting action is performed by dc–dc converters and converting from dc to ac is done by dc–ac inverters. Moreover, in a system, energy storage units, such as a battery and super-capacitor, are required in order to power the auxiliary units in the warming-up stage of fuel cells. In this case, a bidirectional dc–dc converter is additionally implemented to manage the energy storage unit.

Even though there are various combinations of dc–dc converters, bidirectional converters, and dc–ac inverters, they can be grouped into three categories as shown in Fig. 3 and the overall characteristics comparison can be summarized in Table 1. From this comparison, it is noted that the energy storage unit is better connected to the dc-link capacitor in parallel through the bidirectional converter for maximum fuel cell utilization and maintenance of batteries. However,

using a bidirectional converter causes the system cost to be increased and overall system efficiency to be deteriorated. Therefore, according to the applications one should select a proper configuration among these three.

The converter and inverter circuit can be broadly divided into voltage source and current source topologies as shown in Fig. 4.

In the case of the voltage source, it basically uses a bulk capacitor in parallel with a dc-link bus. In this topology, there is no startup problem and it has low switch voltage stress.

Table 1
Comparison of basic configurations of PCS

Type	Advantages	Disadvantages
1	Low cost, no unbalance problem	Poor maintenance of battery, poor utilization of fuel cell
2	Well maintenance of battery	High voltage battery cost, unbalance problem of battery
3	Low voltage battery, no unbalance problem	Cost, complicated control

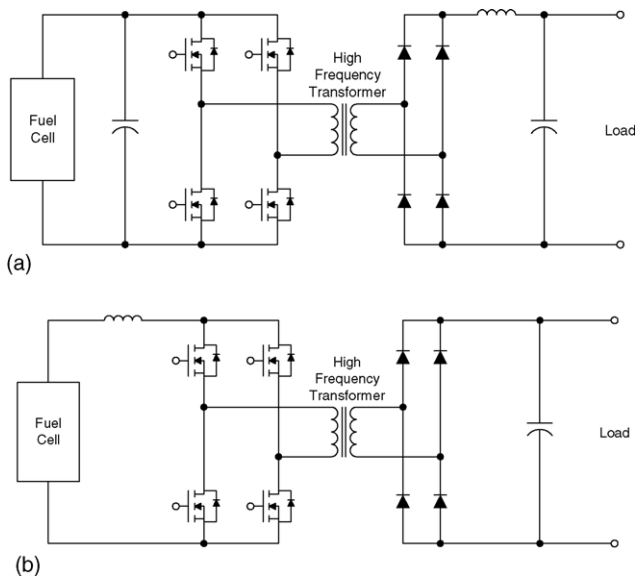


Fig. 4. Comparison of voltage and current source topologies: (a) voltage source and (b) current source.

However, an effective dead-time scheme is needed in order to avoid the shoot-through problem and an output inductor is required to smooth the output voltage ripple. Also, boosting action is up to the transformer's turn ratio, so that it causes poor magnetization utilization. On the other hand, in the case of the current source, it basically uses an input inductor choke in series, but there is no output inductor choke. It cannot start with low output voltage of fuel cells and suffers from high switch voltage stress. Therefore, in practical applications, voltage source and current source topologies are combined for high efficiency and high performance [4,5]. In dc–ac inverters, voltage source inverters have been utilized and are familiar with many researchers. Full-bridge, half-bridge and push-pull topologies are representative ones in voltage source inverters, which are depicted in Fig. 5. Half-bridge inverters are voltage-doubler because the output voltage can be obtained is twice that of input voltage, so that one can get a large voltage gain for the system.

3. Overview of PCS topologies and controls

In this section, various PCS topologies are considered [6–9]. These topologies are based on the report of Future Energy Challenge (FEC) 2003, which is sponsored by SECA, DOE. The FEC is an international university competition in order to develop a low-cost PCS for fuel cells to meet the cost target of \$400/kW in 2010. FEC 2003 gives a design specification for the PCS, including manufacturing cost, efficiency, and package weight for practical applications. This specification is summarized in Table 2 and the PCS designer can refer it as useful data in development.

The PCS as shown in Fig. 6(a) is designed by the Seoul National University of Technology (SNUT) team and was

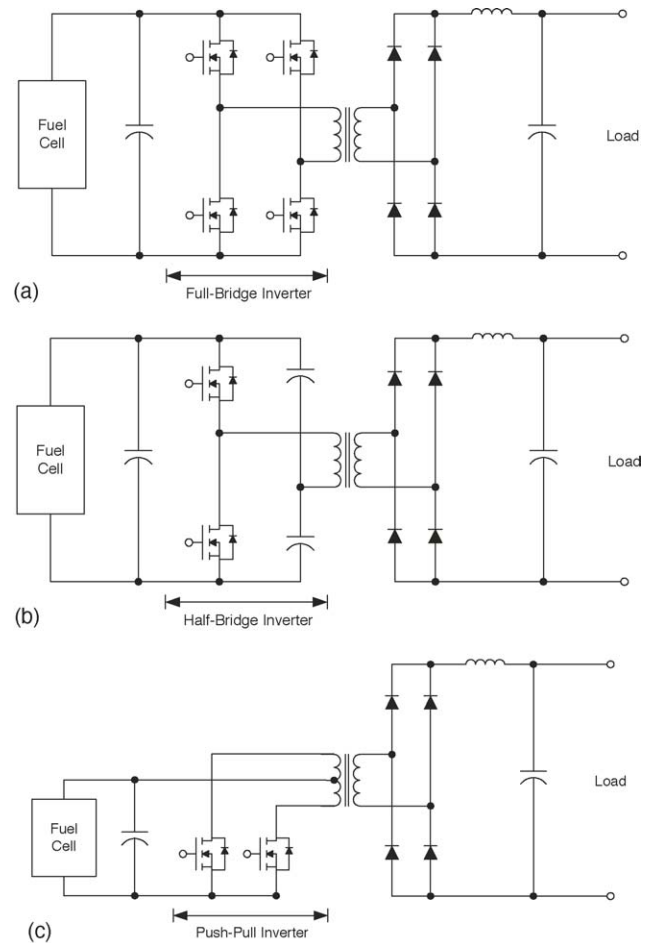


Fig. 5. Various types of voltage source inverters: (a) full-bridge; (b) half-bridge and (c) push-pull.

awarded First Grant Prize. Topologically, it combines a full-bridge converter for boosting up the low voltage of the fuel cell and it is converted to 120 V/240 V_{ac} source by a full-bridge single-phase dc–ac inverter, which was discussed in a previous section in this paper. Also, it includes a bidirectional dc–dc converter to manage the energy storage unit, 48 V battery bank. The front-end full-bridge dc–dc converter is operated at 25 kHz and outputs 400 V_{dc} from 22 to 41 V_{dc}

Table 2
Specification of PCS in 2003 FEC competition

Design items	Minimum target requirement
SOFC (5 kW)	29 V nominal, 22–41 V _{dc} , 275 A max.
Battery	48 V nominal, +10 to –20%, 500 Wh
Output power	Nominal: 5 kW continuous at DPF 0.7 Overload: 10 kW overload for 1 min at DPF 0.7
Output voltage	Split single-phase 120/240 V, 60 Hz Voltage regulation: ±6% Frequency regulation: ±0.1 Hz THD: ≤5%
Manufacturing cost	≤\$60/kW
Efficiency	≥90%
Packing weight	≤30 kg
EMI	FCC 18 Class A

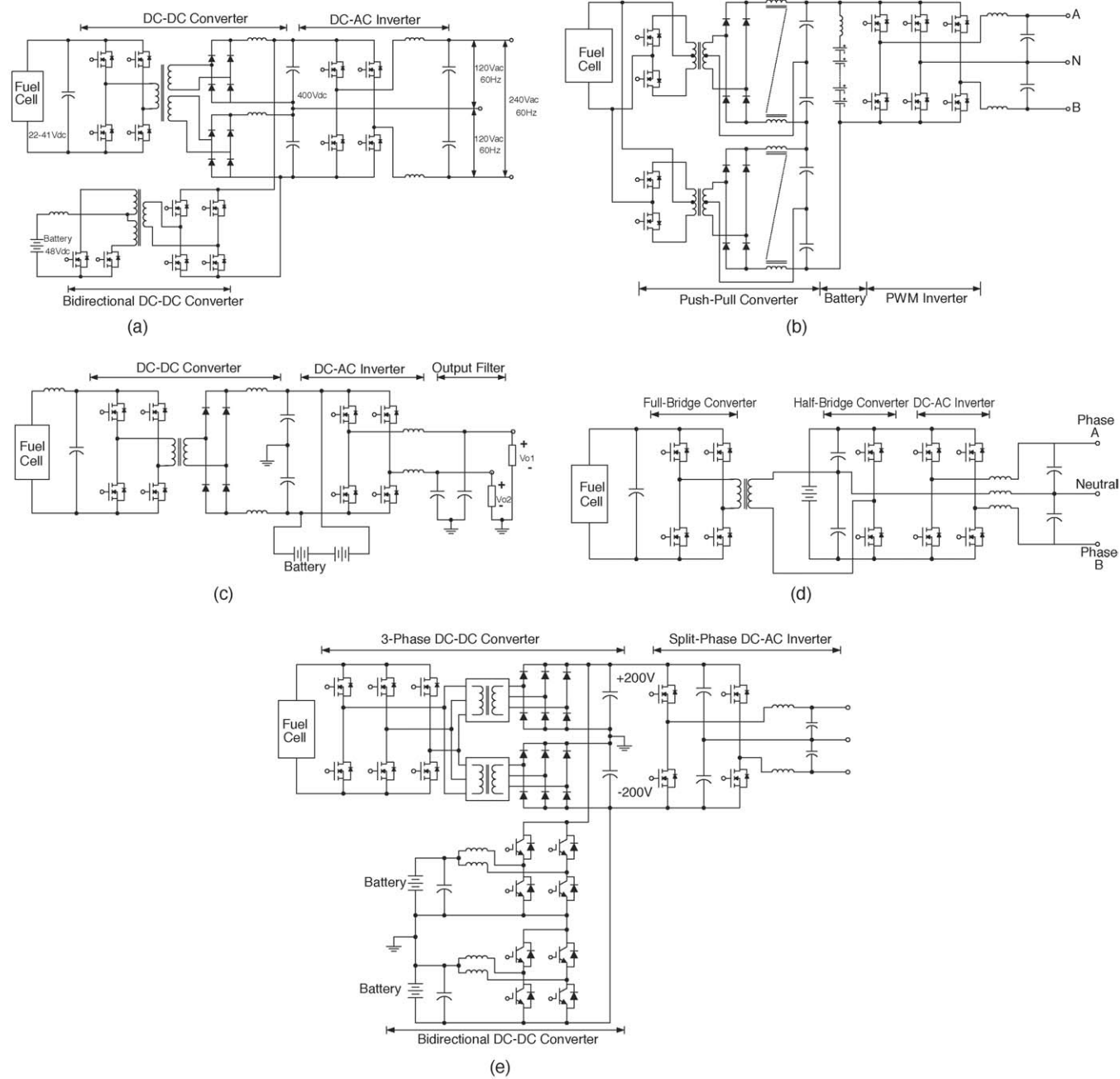


Fig. 6. Various PCS topologies: (a) SNUT; (b) Texas A&M; (c) Wisconsin; (d) MSU and (e) VPEC.

input. And the pwm inverter's switching frequency is 20 kHz as well as the bidirectional converter. In the case of a bidirectional converter, it consists of a full-bridge converter and a push-pull converter and the charging action performed by the full-bridge converter and the push-pull converter handles discharging action.

Texas A&M University proposed a topology in Fig. 6(b). In particular, it contains two push-pull converters, which output 200 V_{dc} at 2.4 kW rating, respectively, and consequently 400 V_{dc} output is obtained. Also, the high-voltage battery is inserted between the dc-link capacitor and inverter, which is one of the basic configurations in Fig. 3. This battery bank consists of 32 batteries of 12 V_{dc} and in order to decrease the inverter ripple current, an inductor is connected in series with the battery bank. As is well known, the inverter ripple current directly affects the fuel cell performance, so that it should be minimized as much as possible.

Basically the topology as shown in Fig. 6(c), which has been proposed by the team of University of Wisconsin, is not distinguishable from the above two topologies. It uses a full-bridge converter and an inverter and a battery bank is inserted between the dc-link capacitor and the inverter.

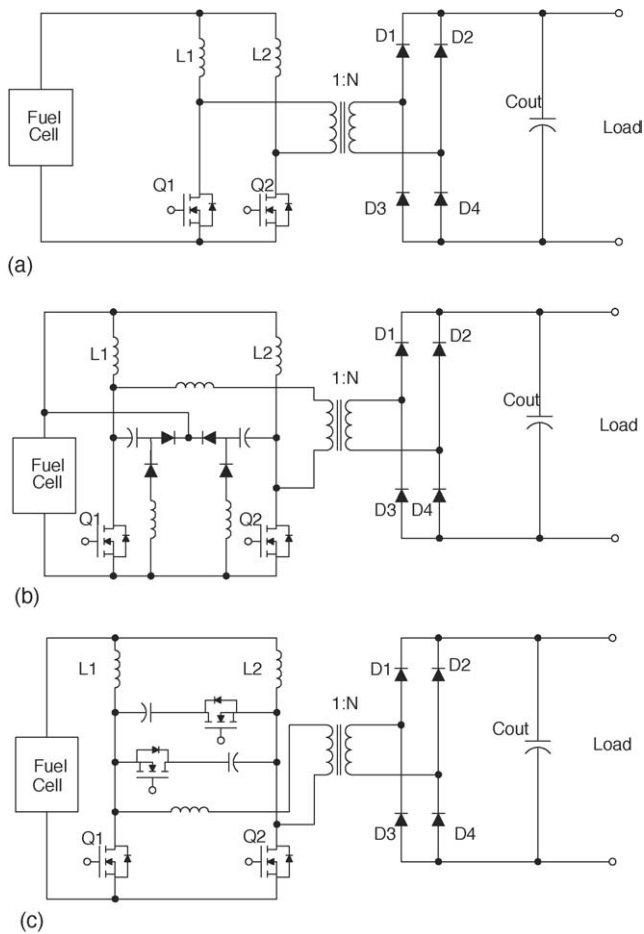
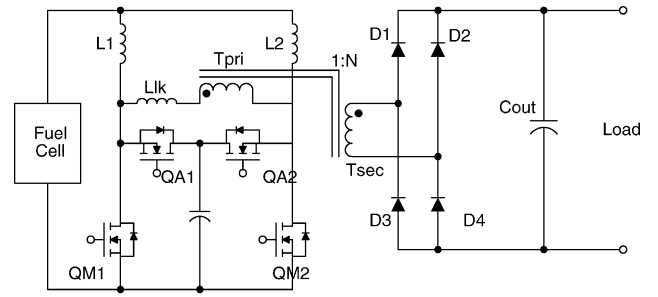
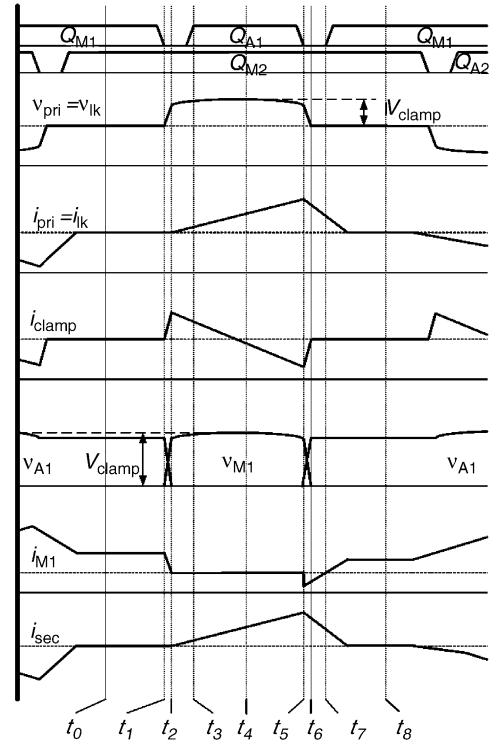


Fig. 7. Variation of current source dc-dc converters: (a) current source half-bridge converter; (b) with lossless snubber and (c) with active lossless snubber.



(a)



(b)

Fig. 8. Proposed active clamped current source converter: (a) configuration and (b) operation modes.

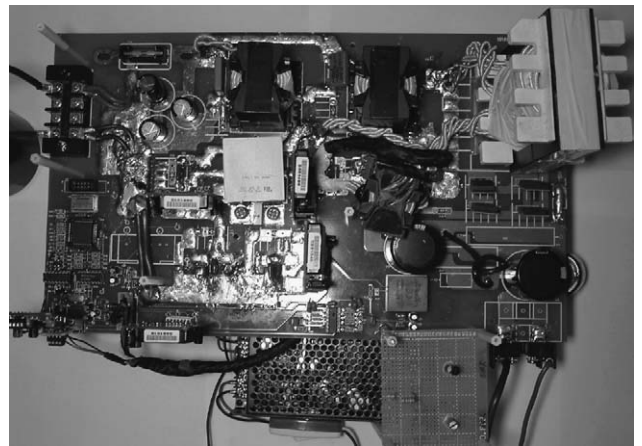


Fig. 9. Experimental prototype of developed active clamped current source converter.

A team from Michigan State University (MSU) uses a half-bridge converter (voltage-doubler) in their system as shown in Fig. 6(d). In order to solve the drawback of conventional full-bridge boost converters, such as drawing large spikes of current from the fuel cell, this team uses the half-bridge converter composed of two capacitors and two MOSFETs. However, it is also noted that this topology can cause the system cost to be increased by using additional switches.

Virginia Polytechnic Institute and State University (VPEC) presented the PCS as shown in Fig. 6(e). It consists of a three-phase dc–dc converter, a split-phase dc–ac inverter, and a push-pull-type bidirectional converter. In the

three-phase dc–dc converter, better current sharing can be obtained, but the auxiliary units, such as gate drive and controller for the switches, become a problem. The bidirectional dc–dc converter operates in discharging when the power flow is from battery to dc-link and on the other hand, when the power flow is from dc-link to battery, it operates in charging.

The detailed operational principles and experimental characteristics are referenced in [6].

4. Proposed PCS for fuel cells

From the above-mentioned topologies, one can understand how the PCS is basically designed and controlled.

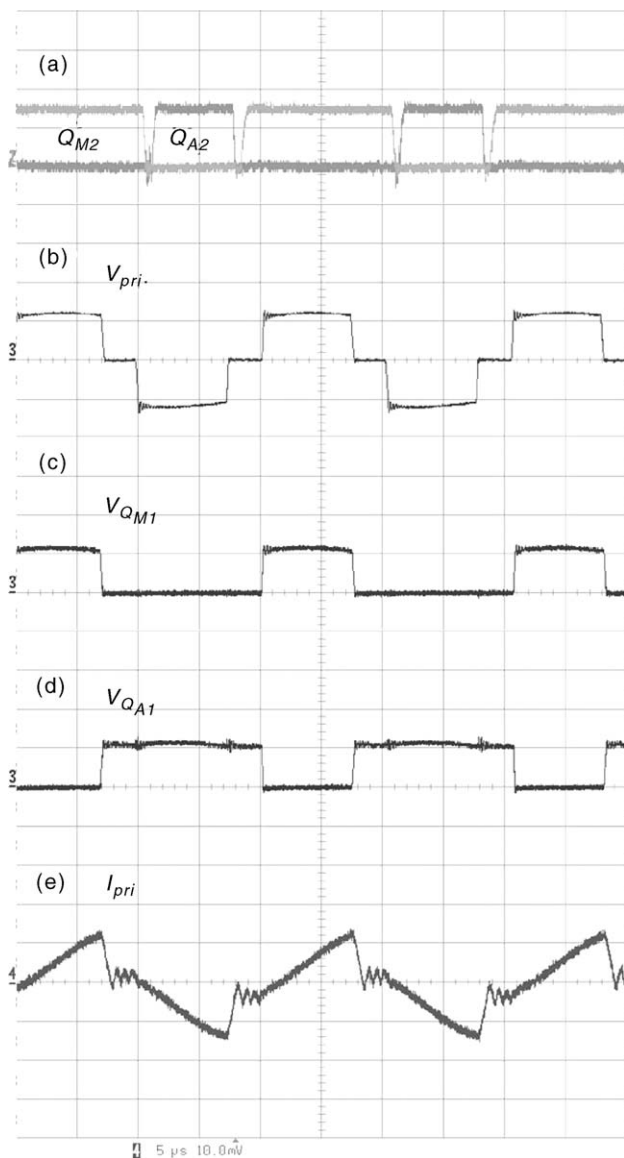


Fig. 10. Experiment voltage and current waveforms of proposed current source converter (time: 5 μ s/div.): (a) gating signals (10 V/div.); (b) transformer voltage at primary side (100 V/div.); (c) voltage across the main switch (100 V/div.); (d) voltage across the auxiliary switch (100 V/div.); (e) transformer current at primary side (10 A/div.).

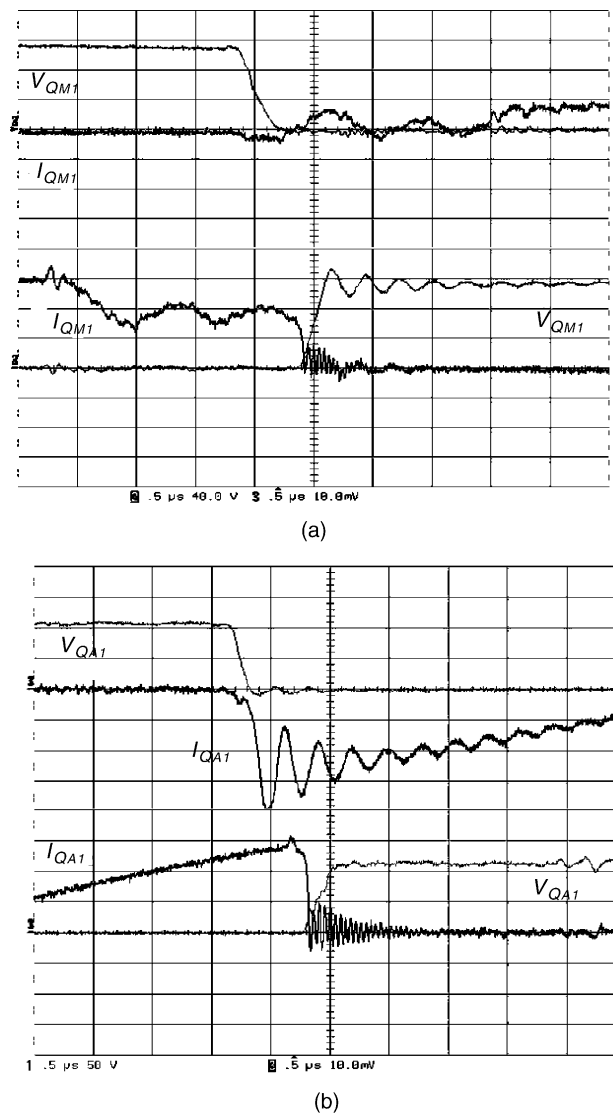


Fig. 11. Zero voltage switching operation of the switches during turn-on/turn-off transients: (a) main switch Q_{M1} (top: turn-on; bottom: turn-off; 40 V/div.; 4 A/div.; 0.5 μ s/div.) and (b) auxiliary switch Q_{A1} (top: turn-on; bottom: turn-off; 50 V/div.; 2 A/div.; 0.5 μ s/div.).

Even though five topologies from different universities are explained as examples, it is noted that the full-bridge, the half-bridge, and the push-pull are fundamentally used and different control schemes are adapted to output better static and dynamic performance.

Based on the conventional PCS topologies, a novel dc–dc converter and a bidirectional converter are proposed in this paper in order to develop a cost-effective and high-performance PCS for battery-fuel cell hybrid systems [10–12].

4.1. An active clamping current-fed half-bridge converter

In fuel cell applications, voltage source converter configurations may not be optimal due to the severe ripple current characteristics. In order to handle the ripple current, a large number of electrolyte capacitors are essentially required, resulting in an increase of the overall system size and manufacturing cost. Moreover, in voltage source converters, a high winding ratio between primary and secondary sides of the high-frequency transformer is necessary because the boosting action is only performed by the winding ratio and also it causes the snubber to be enlarged to handle the surge at turn-off switching. Otherwise, in current source converters, using an inductor decreases the current ripple as well as electrolyte capacitor size. Also, an active boosting action can be achieved with relatively low winding ratio. Therefore, for the fuel cell system, current source converters might be a better choice than voltage source ones. The conventional current source converters have been depicted in Fig. 7. The converter

in Fig. 7(a) provides high conversion ratio, simplicity of construction, reduction of component stress, and minimization of conduction loss. However, it suffers from severe voltage overshoots at turn-off due to the storage energy in the leakage inductor of the transformer. Figs. 7(b) and (c) are converters with lossless snubber, which can solve the inherent problem of the circuit in Fig. 7(a). The main problems of Figs. 7(b) and (c) are that the snubber circuit in Fig. 7(b) only operated at turn-off and its circuit is too complicated and in Fig. 7(c), even though zero voltage switching (ZVS) operation can be achieved both at turn-on and turn-off, the voltages across the auxiliary switches are twice as those of the main switches.

In this paper, a new active clamping current source half-bridge converter is proposed as shown in Fig. 8(a), which can solve the problems of the conventional current source converters. The proposed converter has predominant high boosting output voltage and high efficiency characteristics under the inherently severe low output voltage of the fuel cell through the overall load conditions. The proposed converter consists of a single clamp capacitor (C_{clamp}) and two auxiliary switches (Q_{A1} , Q_{A2}) based on the conventional converter circuit.

The main advantages of the proposed circuit are that ZVS operation of all switches, constant clamping voltage ($=V_{clamp}$) across all switches, and simple gate drive implementation. The switching operation can be divided into two symmetrical half cycles and the circuit has seven operational states during a half switching cycle as shown in Fig. 8(b). The detailed operational principles can be explained as follows:

- Mode 1 ($t_0 < t < t_1$)

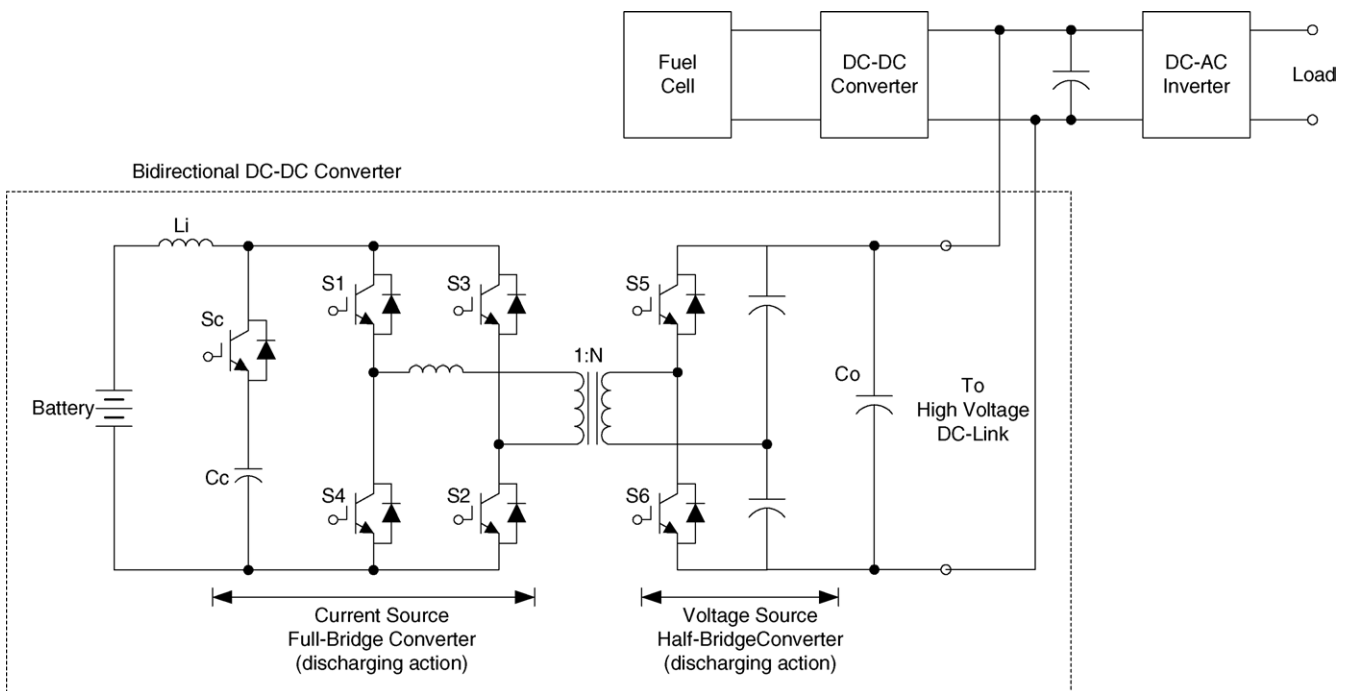


Fig. 12. Proposed bidirectional dc–dc converter.

The main switches Q_{M1} and Q_{M2} are turned on. The energy storages into boost inductors L_1 and L_2 and voltages across the auxiliary switches (Q_{A1} , Q_{A2}) are clamped as V_{clamp} .

- Mode 2 ($t_1 < t < t_2$)

The main switch Q_{M1} is turned off and current I_{L1} flows through parasitic capacitor C_{M1} of V_{M1} . Voltage across C_{M1} (V_{M1}) is rising up to V_{clamp} and V_{A1} of the auxiliary switch Q_{A1} is declining to zero.

- Mode 3 ($t_2 < t < t_3$)

At t_2 , the anti-parallel diode D_{A1} is about to conduct and Q_{A1} can be turned on with zero voltage at this moment.

- Mode 4 ($t_3 < t < t_4$)

The auxiliary switch Q_{A1} is turned on with ZVS. From mode 3 to mode 6, the current i_{clamp} and voltage v_{clamp} can be described by following equations:

$$i_{\text{clamp}}(t) = (I_{L1} - I_{lk0})\cos \omega_0(t - t_2) \quad (2)$$

$$v_{\text{clamp}}(t) = (I_{L1} - I_{lk0})Z_0 \sin \omega_0(t - t_2) + V_0n \quad (3)$$

where angular resonance frequency $\omega_0 = 1/\sqrt{L_{lk}C_{\text{clamp}}}$, characteristic impedance $Z_0 = \sqrt{L_{lk}/C_{\text{clamp}}}$, and initial current condition of leakage inductor is I_{lk0} at t_4 .

- Mode 5 ($t_4 < t < t_5$)

At t_4 , the clamp capacitor starts to transfer the energy into the primary winding during the resonant operation through Q_{A1} . The current of leakage inductor L_{lk} can be expressed

$$i_{lk}(t) = I_{L1} - (I_{L1} - I_{lk0})\cos \omega_0(t - t_2) \quad (4)$$

- Mode 6 ($t_5 < t < t_6$)

The auxiliary switch Q_{A1} is turned off. The parasitic capacitor C_{A1} is charged by leakage inductor current i_{lk} . Voltage across C_{A1} ($=V_{A1}$) is rising up to V_{clamp} and C_{M1} of the main switch Q_{M1} is declining to zero.

- Mode 7 ($t_6 < t < t_7$)

At t_6 , the leakage inductor current i_{lk} discharges to C_{M1} , turns on the anti-parallel diode D_{M1} , and Q_{M1} can be turned on with zero voltage.

$$i_{lk}(t) = -\frac{V_0n}{L_{lk}}(t - t_5) + i_{lk}(t_5) \quad (5)$$

$$i_{DM1}(t) = i_{lk}(t_5) - \frac{V_0n}{L_{lk}}(t - t_5) - I_{L1} \quad (6)$$

A 500 W converter with 48 V input voltage (output voltage of the fuel cell) and 380 V output voltage is designed and implemented as shown in Fig. 9 with the following parameters: inductor 200 μH , leakage inductor 6 μH , clamp capacitor 2 μF , winding ratio 1:3.5, and switching frequency 50 kHz. As explained above, the proposed current source converter has advantage over the voltage source one with respect to winding ratio. In this example, if it is implemented by a voltage source converter, the winding ratio should have 1:14, which makes the transformer be enlarged. The general output characteristics of the proposed converter are displayed in Figs. 10 and 11. From these results, it is noted that the

converter is operated under ZVS condition and the overall efficiency is estimated by 96% as shown in Fig. 11.

4.2. A bidirectional dc–dc converter

In fuel cell generating systems, the energy storage unit is not only required to enhance the transient response time, but also to compensate the peak power demand. For example, in

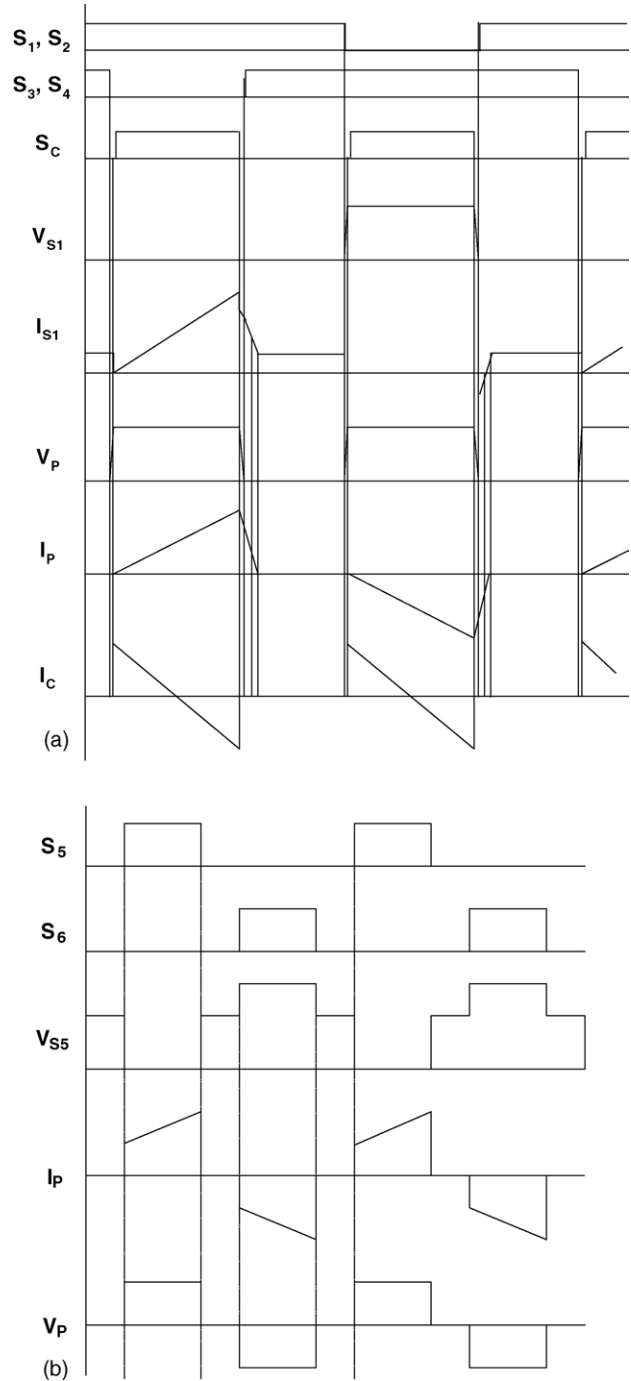


Fig. 13. Timing diagram of (a) discharging (active clamped current source full-bridge converter) and (b) charging (voltage source half-bridge converter).

the residential application, the power is usually about 1 kW in normal use. However, in peak mode, it increases up to 3 kW. In this case, one can design the fuel cell system with a 1 kW fuel cell stack and 2 kW energy storage unit in order to make the overall system cost as low as possible. In this paper, a novel bidirectional dc–dc converter is proposed, which is suitable for battery–fuel cell hybrid applications. As shown in Fig. 12, the proposed converter employs an active clamp current source converter in the low-voltage side (48 V_{dc} battery) for discharging and a voltage source half-bridge converter in the high-voltage side (inverter dc-link) for charging. The advantages of the proposed bidirectional converter can be addressed as:

- The voltage across the switches is well clamped;
- There is no voltage overshoot;
- All switches operate with ZVS;
- No ancillary snubbing is required in either primary or secondary;
- Transformer leakage inductance, while instrumental for ZVS attainment does not significantly interfere with the circuit operation.

The algorithms for discharging and charging are depicted in Fig. 13 and the overall operational principles are summarized as

- Discharging mode
 - Reference voltage limits 375 V dc-link voltage;
 - Instantaneous discharge when reference voltage is decreased under 375 V_{dc};
 - Monitoring battery capacity.
- Charging mode
 - In light load, battery is charged;
 - Battery capacity is less than the set value.

Fig. 14 shows the experimental set-up of the proposed bidirectional converter and the overall performance can be examined by the voltage and current waveforms in Fig. 15. From the experimental results, it is noted that voltage across all switches and the primary side of the transformer are clamped to the same value of clamping capacitor and with the help of the lossless snubber, the overshoot voltages of all switches

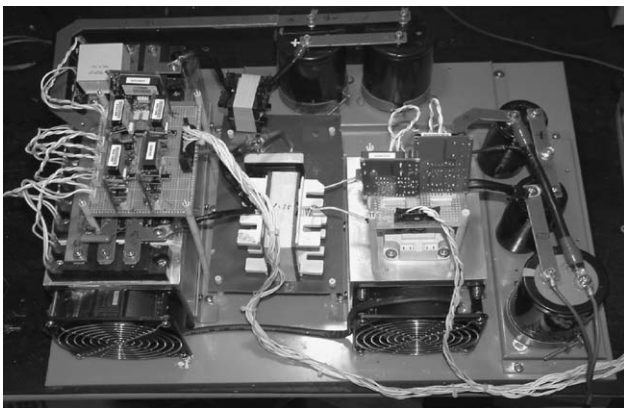


Fig. 14. Experimental set-up of proposed bidirectional converter.

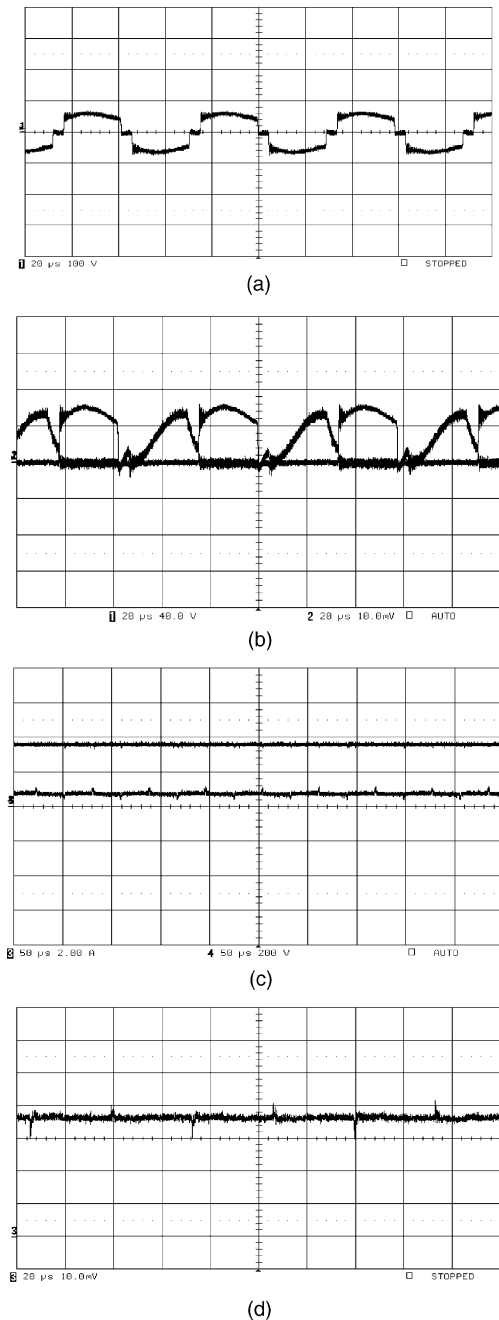


Fig. 15. Overall characteristics of proposed bidirectional converter: (a) transformer primary voltage (low side) (100 V/div., 20 μs/div.); (b) switch voltage and current (40 V/div., 10 A/div., 20 μs/div.); (c) discharging voltage and current (200 V/div., 2 A/div., 50 μs/div.) and (d) charging current (0.1 A/div., 20 μs/div.).

could be successfully eliminated. Also, it can be certified that it performs the charging and discharging action according to the control values.

5. Conclusions

In this paper, a general design approach of the PCS for fuel cell generation systems is studied with the help of several

PCS examples. From this study, it is noted that full-bridge, half-bridge and push-pull converters are fundamentally used and various different topologies can be derived. Also, the comparison of the voltage source and current source topologies has been done, so that a system designer can select the proper topology according to the applications. Moreover, in this paper, a cost-effective and high-performance dc–dc converter and bidirectional converter for battery-fuel cell hybrid systems have been proposed and their performance has been tested. From the results, it is expected that this paper can be utilized by the PCS designer for typical fuel cell applications considering cost and performance issues.

References

- [1] J. Larminie, A. Dicks, *Fuel Cell Systems Explained*, 2nd ed., Wiley, 2003, pp. 45–66.
- [2] B.-K. Lee, B. Fahimi, M. Ehsani, *IEEE Power Electronics Specialist Conference*, 2001, pp. 2019–2024.
- [3] B.-K. Lee, M. Ehsani, *IEEE Applied Power Electronics Conference*, 2003, pp. 277–280.
- [4] H.W. Van Der Broeck, J.D. Van Wyk, *IEEE Trans. Ind. Appl.* (1984) 309–320.
- [5] O. Stihl, B.T. Ooi, *IEEE Trans. Power Electron.* (1988) 453–459.
- [6] *Future Energy Challenge 2003 Report*, 2003.
- [7] P. Enjeti, M.H. Todorovic, L. Palma, *Proceedings of 2004 Fuel Cell Seminar*, 2004.
- [8] J. Lai, M. Schenck, K. Stanton, *Proceedings of 2004 Fuel Cell Seminar*, 2004.
- [9] K. Wang, F.C. Lee, J. Lai, *IEEE Applied Power Electronics Conference*, 2000, pp. 111–118.
- [10] J.T. Kim, B.-K. Lee, T.W. Lee, S.J. Jang, S.H. Kim, S.S. Kim, C.-Y. Won, *IEEE Power Electronics Specialist Conference*, 2004, pp. 4709–4714.
- [11] S.J. Jang, T.W. Lee, W.C. Lee, C.-Y. Won, *IEEE Power Electronics Specialist Conference*, 2004, pp. 4722–4728.
- [12] T.W. Lee, B.-K. Lee, C.-Y. Won, *IEEE Power Electronics Specialist Conference*, 2004, pp. 4743–4748.